Acta Cryst. (1988). B**44**, 495–502

Study of the Modulated Phase of $(C_3H_7NH_3)_2CdCl_4$ by Single-Crystal X-ray Diffraction

BY BERNARD DOUDIN AND GERVAIS CHAPUIS

Université de Lausanne, Institut de Cristallographie, BSP Dorigny, 1015 Lausanne, Switzerland

(*Received 5 January* 1988; *accepted 6 April* 1988)

Abstract

Bis(*n*-propylammonium) tetrachlorocadmate shows a modulated phase stable between two orthorhombic phases on the temperature scale. The superspace group could be determined unambiguously on the basis of the selection rules. In addition to Bragg main reflections, 1137 first-order and 107 second-order satellites with an intensity larger than 3σ were measured. The refinement revealed a displacive modulation of harmonic type. The $CdCl_6$ octahedra show modulation amplitudes larger than 0·2 Å. To a first approximation, the dynamics of the octahedra can be analyzed in terms of a rotation about the *a* axis and a translation along the *c* axis. The low-temperature phase can be considered as a lock-in of the modulated one with a change of **q** from 0·42**b*** to 1**b***. In this phase the rotation of the octahedra about **a** is frozen and a unique hydrogen-bonding scheme is adopted between the alkylammonium ion and the Cl atoms. For the modulated phase, $M_r = 374{\cdot}5$, superspace group $P^{Abma}_{s\bar{1}1}(0,\beta,0)$, $a = 7{\cdot}585$ (5), $b = 7{\cdot}359$ (1), $c = 25{\cdot}053$ (6) Å, $V = 1398$ (1) Å^3, $Z = 2$ (primitive cell), Mo $K\bar{\alpha}$, $\lambda = 0{\cdot}71069$ Å, $\mu = 22{\cdot}5$ cm^{-1}, $wR(F) = 0{\cdot}072$ for 1791 independent reflections [$wR(F) = 0{\cdot}088$ for first-order satellites].

1. Introduction

The aim of this work is to present a study of the structural phase transitions of $(C_3H_7NH_3)_2CdCl_4$ by single-crystal X-ray diffraction and to propose a possible mechanism for the onset of the modulated phase. Three transitions have been detected at approximately 180, 158 and 110 K (Blinc *et al.*, 1977; Chapuis, 1978; White, Granville, Davies & Staveley, 1981; Mokhlisse, Couzi, Chanh, Haget, Hauw & Meresse, 1985). In a previous investigation (Chapuis, 1978) two phases were analyzed by single-crystal diffraction: an orthorhombic room-temperature (ORT) phase with space group *Abma* and a second orthorhombic low-temperature (OLT) phase with space group *Pbca*, believed to be stable below the transition at 180 K. Raman scattering and X-ray diffraction studies by Mokhlisse *et al.* (1985) showed that the OLT phase appears only below 158 K. Our present X-ray investigations revealed the presence of an intermediate modulated phase. The symmetry of the average structure (based on main reflections only) is also *Abma*. The modulation vector of the satellite reflections is $\mathbf{q} = 0{\cdot}418$ (5)**b***.

$$\mathrm{ORT}(Abma) \overset{\approx 180\ \mathrm{K}}{\longleftrightarrow} \mathrm{INC}(Abma,\ \mathbf{q} \cong 0{\cdot}42\mathbf{b}^*) \overset{\approx 158\ \mathrm{K}}{\longleftrightarrow} \mathrm{OLT}(Pbca)$$

This phase has strong similarities with the incommensurate phase ε appearing at low temperature in the homologous Mn compound $(C_3H_7NH_3)_2MnCl_4$ (Depmeier & Mason, 1982). The presence of an incommensurate transition in a perovskite-type layer structure is thus not unique.

2. Experimental

2.1. *Synthesis*

The synthesis of the compound is similar to that reported for the corresponding Mn compound (Arend, Hofman & Waldner, 1974). Single crystals were grown on the surface of an aqueous solution and mounted directly on a glass fiber.

2.2. *X-ray measurements*

X-ray diffraction measurements were performed on a CAD-4 four-circle diffractometer. The three phases were measured at approximately 210, 153 and 130 K. The temperature was constant within a range of 0·2 K. An open stream of nitrogen gas (modified Enraf–Nonius system) was used and the temperature monitored by a thermocouple placed a few millimeters from the crystal. The thermocouple indicates a temperature a few degrees lower than that of the crystal.

2.3. *Crystal data*

Two samples of dimensions 0·5 × 0·22 × 0·05 and 0·62 × 0·26 × 0·11 mm were used for the measurements. The ω–2θ scan procedure with Mo $K\bar{\alpha}$ radiation (graphite monochromator) was applied. Table 1 gives a summary of the data-collection parameters.

*XRAY*72 (Stewart, Kruger, Ammon, Dickinson & Hall, 1972) was used for the conventional structures, *REMOS*85.0 (Yamamoto, 1982) for the modulated phase. Atomic scattering factors were calculated according to Cromer & Mann (1968). Anomalous-dispersion corrections for Cl and Cd atoms were taken from Cromer & Liberman (1970). An absorption correction was applied with linear absorption coefficient

0108-7681/88/050495-08$03.00

Table 1. *Parameters used for data collection*

Scan width (°)	0·50 + 0·45 tanθ
Scan speed (° min^{-1})	1·42, 0·18 for satellites
Range of *hkl*	$0 \le h \le 8, 0 \le k \le 9, -27 \le l \le 27$
$(\sin\theta/\lambda)_{max}$ (Å^{-1})	0·55 ($2\theta_{max} = 45·0°$)
Standard reflections	(0,4,10) (2,4,8) ($\bar{2}$,4,8) (no intensity variation with time observed)

	Room temp.	Incommensurate	Low temp.
Non-equivalent reflections	507	3284	945
$I \ge 3\sigma$	435	1791	715

$\mu = 22·5$ cm^{-1}. R factors result from a full-matrix least-squares refinement and are calculated as $[\sum w(F^2)(F^2_{obs.} - F^2_{calc.})^2/\sum w(F^2)F^2_{obs.}]^{1/2}$ with $w(F^2) = 1/\sigma^2(F^2_{obs.})$ for *XRAY*72 and $[\sum w(F)(|F_{obs.}| - |F_{calc.}|)^2/\sum w(F)F^2_{obs.}]^{1/2}$ with $w(F) = 1/\sigma^2(F_{obs.})$ for *REMOS*85.0. σ derives from counting statistics.*

3. The ORT and OLT structures

The results are in agreement with those published by Chapuis (1978). Lattice parameters (20 reflections centred at 2θ angles between 30 and 40°) were as follows:

	ORT phase	INC phase	OLT phase
Measurement temperature (K)	210·0 (2)	153·0 (2)	130·5 (2)
Axis length (Å)			
a	7·607 (3)	7·585 (5)	7·568 (5)
b	7·370 (3)	7·359 (1)	7·359 (1)
c	25·184 (6)	25·053 (6)	25·515 (8)
Volume (Å^3)	1412 (1)	1398 (1)	1421 (1)

Considering the primitive cell, $Z = 2$ for the ORT and INC phases; in the OLT phase, $Z = 4$.

Figs. 1 and 2 show the essential differences between the two orthorhombic structures. $(C_3H_7NH_3)_2CdCl_4$ is formed by successive layers of corner-sharing $CdCl_6$ octahedra. In the cavities the ammonium end of the chain is connected by hydrogen bonds to one equatorial and two axial Cl atoms (called respectively Cl_e and Cl_a). The methyl end has van der Waals interactions with the chains attached to the adjacent $CdCl_4$ layer. At room temperature, only one H atom was found in a difference Fourier map. As a result of symmetry constraints, the C and N atoms lie on the mirror plane perpendicular to the **b** direction. Consequently, two possible N—H···Cl bonding schemes are possible. At low temperature this disorder is frozen and each chain adopts a unique hydrogen-bond scheme.

The propylammonium ion is also disordered. In the ORT phase, surprisingly short C—C distances and large anisotropic displacements appear mainly along the **b** direction. An attempt to split C(1) and C(2) in order to improve the model has been undertaken. With isotropic displacement parameters the difference Fourier synthesis gives, however, higher residual peaks near these positions (~1 e Å^{-3}). Even at low temperature the C(2) atom also shows a large displacement along the **b** direction. Results of the structure refinement deduced from main reflections of the INC phase measured at 153 K are also presented. No strong differences have been detected with respect to the ORT phase. Small increases in thermal coefficients were observed. Table 2 gives a summary of the two proposed models.

From the orientation of the octahedra, it is easy to deduce the type of connection of the organic chain to the $CdCl_4$ layers. At room temperature, the tilting of the octahedra about the **b** axis favours the hydrogen bond formed by the only H atom observed on a difference Fourier map. The rotation about the *a* axis is hindered at the onset of the low-temperature phase. It can be expected that the tilt of the rotation about **c** will reduce the disorder of the C(2) and the displacement of Cl_e atoms in the *ab* plane. No investigations of the phase

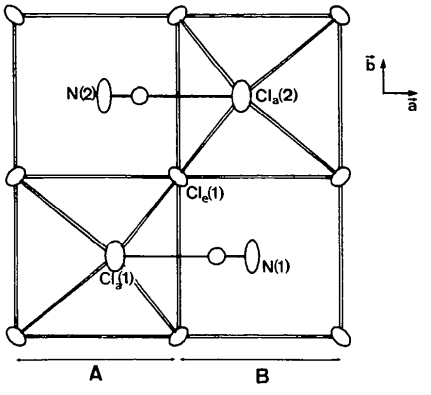

Fig. 1. *ab* projection of the ORT phase. N and Cl atoms are represented with 50% thermal ellipsoids. Cd and C atoms are omitted for clarity. One H atom contributing to the hydrogen bond is indicated. Column *B* is related to column *A* by $\{m_x|\frac{1}{2},\frac{1}{2},0\}$.

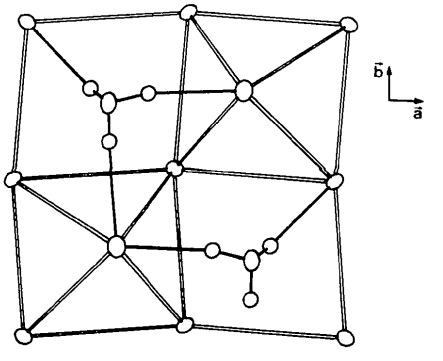

Fig. 2. *ab* projection of the OLT phase. N and Cl atoms are represented with 50% thermal ellipsoids. Cd and C atoms are omitted for clarity (see Fig. 1 for atom labels). H atoms connected to Cl are indicated.

* Lists of structure factors have been deposited with the British Library Document Supply Centre as Supplementary Publication No. SUP 44919 (39 pp.). Copies may be obtained through The Executive Secretary, International Union of Crystallography, 5 Abbey Square, Chester CH1 2HU, England.

Table 2. *Comparison of models for the disorder of the n-propylammonium chains*

Population parameters, fractional coordinates, displacement parameters along **b** and interatomic distances N–C(1), C(1)–C(2), C(2)–C(3) are indicated. $|\Delta\rho|_{max}$ indicates the maximum absolute value of the height found in a difference Fourier map. $(\Delta/\sigma)_{max}$ is the maximum shift over e.s.d. of the refined parameters in the last stage of the refinement.

	pp	x	y	z	U_{22} or U(Å^2)	Distance (Å)
ORT						
N	1·0	0·473 (2)	0·00	0·0852 (5)	U_{22} = 0·055 (10)	
C(1)	0·5	0·574 (2)	0·041 (4)	0·1362 (7)	U = 0·039 (7)	1·53 (2)
C(2)	0·5	0·496 (3)	−0·056 (3)	0·1840 (6)	U = 0·056 (8)	1·52 (3)
C(3)	1·0	0·609 (3)	0·00	0·2315 (6)	U_{22} = 0·096 (19)	1·53 (3)
	R = 3·4%	wR = 5·3%	$\|\Delta\rho\|_{max}$ = 1·0 e Å^{-3}	$(\Delta/\sigma)_{max}$ = 0·009		
N	1·0	0·473 (2)	0·00	0·0855 (5)	U_{22} = 0·056 (9)	
C(1)	1·0	0·570 (3)	0·00	0·1371 (8)	U_{22} = 0·119 (23)	1·50 (3)
C(2)	1·0	0·497 (4)	0·00	0·1829 (7)	U_{22} = 0·291 (42)	1·28 (3)
C(3)	1·0	0·610 (3)	0·00	0·2318 (7)	U_{22} = 0·097 (19)	1·50 (3)
	R = 3·5%	wR = 5·2%	$\|\Delta\rho\|_{max}$ = 0·8 e Å^{-3}	$(\Delta/\sigma)_{max}$ = 0·008		
INC						
N	1·0	0·473 (1)	0·00	0·0847 (3)	U_{22} = 0·070 (7)	
C(1)	0·5	0·573 (2)	−0·040 (4)	0·1336 (5)	U = 0·034 (4)	1·49 (2)
C(2)	0·5	0·499 (2)	0·056 (3)	0·1829 (4)	U = 0·062 (5)	1·50 (2)
C(3)	1·0	0·614 (2)	0·00	0·2315 (5)	U_{22} = 0·097 (13)	1·57 (2)
	R = 3·6%	wR = 4·6%	$\|\Delta\rho\|_{max}$ = 1·1 e Å^{-3}	$(\Delta/\sigma)_{max}$ = 0·037		
N	1·0	0·473 (1)	0·00	0·0846 (3)	U_{22} = 0·072 (7)	
C(1)	1·0	0·572 (2)	0·00	0·1346 (5)	U_{22} = 0·148 (17)	1·48 (2)
C(2)	1·0	0·499 (3)	0·00	0·1818 (6)	U_{22} = 0·342 (35)	1·32 (2)
C(3)	1·0	0·611 (2)	0·00	0·2316 (5)	U_{22} = 0·093 (13)	1·52 (2)
	R = 3·4%	wR = 4·4%	$\|\Delta\rho\|_{max}$ = 0·8 e Å^{-3}	$(\Delta/\sigma)_{max}$ = 0·033		
OLT						
N	1·0	0·4757 (7)	0·024 (2)	0·0862 (2)	U_{22} = 0·025 (4)	
C(1)	1·0	0·5743 (9)	−0·031 (1)	0·1343 (3)	U_{22} = 0·040 (5)	1·52 (1)
C(2)	1·0	0·4897 (9)	0·041 (1)	0·1827 (2)	U_{22} = 0·105 (8)	1·51 (1)
C(3)	1·0	0·6025 (10)	−0·018 (19)	0·2299 (3)	U_{22} = 0·062 (6)	1·57 (1)
	R = 2·5%	wR = 2·5%	$\|\Delta\rho\|_{max}$ = 0·6 e Å^{-3}	$(\Delta/\sigma)_{max}$ = 0·013		

below 110 K could be performed with monocrystals owing to the transformation of the sample into powder at this transition.

4. The modulated structure

Preliminary observations of the intermediate phase were made using Weissenberg photographs. Satellites appeared in addition to the reflections observed at high temperature. The modulation vector **q** is parallel to **b***. The value of 0·418 (5)**b*** was obtained from diffractometer measurements by centering some strong satellite reflections. The width of satellite reflections was similar to the main reflections (≤0·2° for the width at half height of an ω scan). The intensity of the satellites does not vary with time, but strongly increases on lowering the temperature (see Fig. 3). No variation of $|\mathbf{q}|$ has been observed with temperature. Its value is equal to $5/12|\mathbf{b}^*|$ within errors. We can consider this phase as a superstructure, but the term incommensurate is chosen by analogy with the ε phase of the Mn compound. Even if the phase is commensurate, it is appropriate to use the modulated structure formalism for this structure analysis.

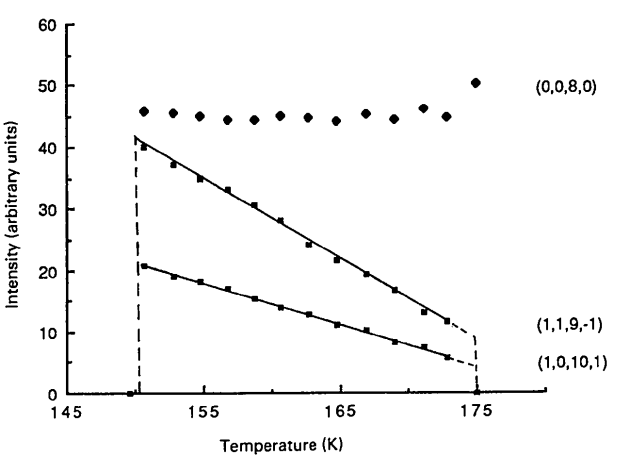

Fig. 3. Temperature variation of some intensities within the INC phase interval. A scale factor was applied to reduce the intensity of the (0,0,8,0) reflection.

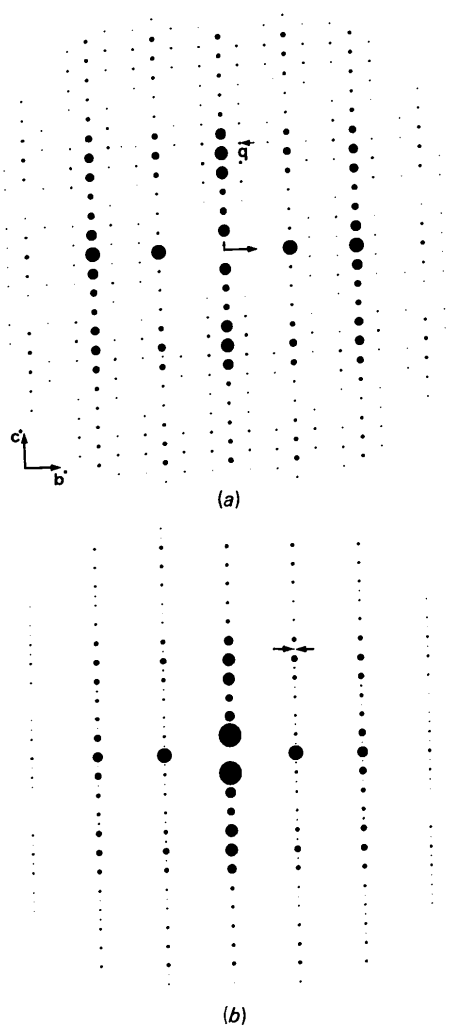

Fig. 4. (*a*) Representation of the 0,*k*,*l*,*m* reciprocal lattice plane of the INC phase. The radius is proportional to $|F_{obs.}|$ (from Yamamoto, 1987). The 0,*k*,*l* plane of the ORT phase is similar to the main reflections of INC phase. (*b*) Representation of the 0,*k*,*l* plane of the OLT phase. Arrows indicate the change of **q** in the lock-in transition.

4.1. *Symmetry*

Abma remains the space group of main reflections, which is in accordance with a second-order phase transition (Heine & Simmons, 1987). Four superspace groups can be considered (de Wolff, Janssen & Janner, 1981), namely:

$$P^{Abma}_{1\bar{1}\,1},\ P^{Abma}_{s\bar{1}\,1},\ P^{Abma}_{1\bar{1}\,s},\ P^{Abma}_{s\bar{1}\,s}.$$

The presence of satellite reflections of the type $h,k,0, \pm 1$ for $k = 2n$ and the absence of reflections of the type $0,k,l, \pm 1$ for $k=2n$ (see Fig. 4), observed for first-order satellites, determined the superspace group unambiguously as $P^{Abma}_{s\bar{1}\,1}$ $(0,\beta,0)$, which has the following reflection conditions:

h,k,l,m	$k + l = 2n$
$0,k,l,m$	$k + m = 2n,\ l = 2n$
$h,k,0,m$	$h = 2n,\ k = 2n$
$h,0,0,m$	$h = 2n$
$0,k,0,m$	$k + m = 2n$
$0,0,l,m$	$l = 2n.$

The generating elements for the superspace group are the following:

$$\{m_x|\tfrac{1}{2},\tfrac{1}{2},0,\tfrac{1}{2}\},\ \{\bar{m}_y|0,\tfrac{1}{2},\tfrac{1}{2},\tfrac{1}{2}\},\ \{m_z|\tfrac{1}{2},0,\tfrac{1}{2},0\}$$
$$\{E|1,0,0,0\},\ \{E|0,-\tfrac{1}{2},\tfrac{1}{2},0\},\ \{E|0,\tfrac{1}{2},\tfrac{1}{2},0\},\ \{E|0,0,0,1\}.$$

These extended symmetry operations act on the superspace R^4. The rotational part is a 4×4 matrix formed by the usual 3×3 matrix in R^3 and an R_{44} element corresponding to the action of the 3×3 matrix on the modulation vector $\mathbf{q}$ (equal to ± 1). The minus sign is shown by a bar over the rotational part. The t_x, t_y, t_z translations are components of a usual translation in R^3, τ is the phase translation of the modulation. The translation $\tau = \frac{1}{2}$ connected to m_x characterizes the symbol s in the superspace group. $\tau = \frac{1}{2}$ connected to m_y fixes the origin of the phase. We chose it to generate an inversion center at the origin of the form $\{\bar{1}|0,0,0,0\}$.

4.2. *Description of a modulated structure and its refinement*

A one-dimensional modulated structure is described by a distortion of a basic (or fundamental) structure having the form of a plane wave with wavevector $\mathbf{q}$. The modulated atomic positions and their probability of occupation are expressed in terms of the Fourier series:

$$x_i^\mu(\bar{x}_4^\mu) = \bar{x}_i^\mu + \left[\tfrac{1}{2}\sum_{n=0}^{\infty} U_{i,n}^\mu \exp(2\pi i n \bar{x}_4^\mu) + \text{c.c.}\right] = \bar{x}_i^\mu + u_i^\mu$$

$$P^\mu(\bar{x}_4^\mu) = \tfrac{1}{2}\sum_{n=0}^{\infty} P_n^\mu \exp(2\pi i n \bar{x}_4^\mu) + \text{c.c.}$$

c.c denotes the complex conjugate; $\bar{x}_i^\mu$ with $i = 1, 2, 3$ is the ith component of the position of the μth atom in the basic structure; $U_{i,n}^\mu$ and $\mathbf{P}_n^\mu$ are the complex amplitudes of the nth-order harmonic (Yamamoto, 1982).

A usual hypothesis is to truncate the series beyond the first-order term to obtain the harmonic approximation. So, for a displacive modulation:

$$x_i^\mu(\bar{x}_4^\mu) = \bar{x}_i^\mu + U_{i,0}^\mu + \text{Re}(U_{i,1}^\mu)\cos(2\pi\bar{x}_4^\mu) - \text{Im}(U_{i,1}^\mu)\sin(2\pi\bar{x}_4^\mu).$$

In this case, nine positional parameters have to be refined for each atom. For this particular structure, the seven non-H atoms are all in special positions. Cl_a, N, C(1), C(2), C(3) lie on the mirror plane perpendicular to **b**. If atom ν is related to atom μ by $\{\bar{m}_y|0,0,0,\frac{1}{2}\}$, we have:

$$u_i^\nu = u_i^\mu(-\bar{x}_4^\mu + \tfrac{1}{2}) \qquad i = 1,3$$
$$u_2^\nu = -u_2^\mu\,(-\bar{x}_4^\mu + \tfrac{1}{2}).$$

If atoms ν and μ are identical, we have:

$$\text{Im}(U_{i,1}^\mu) = 0 \qquad i = 1,3$$

and

$$U_{2,0}^\mu = \text{Re}(U_{2,1}^\mu) = 0.$$

Taking into account the invariance of the Cd atom under $\{2_y|0,0,0,\frac{1}{2}\}$ and $\{\bar{m}_y|0,0,0,\frac{1}{2}\}$ and the invariance of Cl_e under $\{2_z|\frac{1}{2},\frac{1}{2},0,0\}$, a total of 31 independent positional parameters remain.

Atomic displacement components U_{ij} have the same meaning as for conventional structures and are used in a Debye–Waller factor of the form:

$$\exp\left(-2\pi^2 \sum_{i=1,3}\sum_{j=1,3} U_{ij}\,\mathbf{a}_i^*.\mathbf{a}_j^* h_i h_j\right).$$

In addition, 28 thermal parameters have to be refined.

4.3. *Refinement procedure*

A set of 1791 independent reflections with intensity larger than 3σ were used in the *REMOS*85.0 refinement procedure. The reflections were corrected for absorption and Lorentz–polarization effects. Weights were chosen as $1/\sigma^2(F)$. The integrals in the structure factors were calculated by the Gaussian method using ten divisions. The following residual values were obtained:

	No. of reflections	R	wR
All	1791	0·076	0·072
Main	547	0·044	0·043
First-order satellites	1137	0·090	0·088
Second-order satellites	107	0·216	0·235

The model proposed is a displacive and harmonically modulated structure. Several other models were considered:

(*a*) A modulation of the occupation of the two hydrogen-bonding schemes was tested. It corresponds to the splitting of C(1) and C(2) atoms as proposed in the high-temperature phase. In this model, atoms μ and

v are related by the mirror plane perpendicular to **b** and with probabilities:

$$P^{\mu}(\bar{x}_4^{\mu}) = \tfrac{1}{2} + P_1^{\mu} \sin(2\pi i \bar{x}_4^{\mu})$$
$$P^{\nu}(\bar{x}_4^{\mu}) = \tfrac{1}{2} - P_1^{\mu} \sin(2\pi i \bar{x}_4^{\mu}).$$

Attempts to split C(1) and C(2) or the whole alkylammonium chain gave unsatisfactory results. Specifically, the magnitude of P_1^{μ} was less than $2\sigma(P_1^{\mu})$ and no significant decrease of R was observed in spite of the larger number of refined parameters.

(*b*) As the nth harmonic in the Fourier decomposition of the modulation contributes essentially to the intensity of satellites of order $m \leq n$ (Paciorek & Kucharczyk, 1985), the Fourier series is usually truncated after the term corresponding to the highest order of satellites observed. In our case, a refinement with second-harmonic components was tested. A decrease of the R factor for first-order satellites down to 0·075 is due to the larger number of parameters. For second-order satellites, however, the R factor is 0·45. This is probably due to the very weak observed satellites with $m = \pm 2$. Even in the harmonic approximation, more than ~80% of the calculated structure factors are higher than the observed ones. Considering the nonobserved second-order satellites, the hypothesis of a second-harmonic component is not acceptable: it implies calculated intensities that are too large when compared with observations. In the harmonic approximation, the R factor of 0·23 for second-order satellites is satisfactory considering the small values of the measured intensities.

(*c*) A possible explanation for the low intensity of second-order satellites is a fluctuation in phase and amplitude of the modulation wave (Overhauser, 1971; Axe, 1980). A model of phase fluctuation having a Gaussian distribution is equivalent to a supplementary displacement parameter (Yamamoto, Nakazawa, Kitamura & Morimoto, 1984).

$$F(h,k,l,m) = F^0(h,k,l,m) \exp(-2\pi^2 \Delta t^2 m^2),$$

where $F^0(h,k,l,m)$ is the structure factor when no phase fluctuations are taken into account and Δt is the standard deviation of the phase fluctuation. This parameter was found to converge to approximately zero in a refinement without decreasing the R factors. The phase fluctuation was therefore neglected.

5. Discussion

5.1. *Disorder of the octahedra layers*

The main contribution to satellite intensities is from the modulation of $CdCl_6$ octahedra. The Cd and Cl atoms have displacement amplitudes essentially along the c axis. The axial Cl_a atoms show another displacement along **b** (see Table 3).

It is possible to express these displacements with a model consisting of a rotation φ of the octahedra around **a** with a uniform shift along **c** (see Fig. 5). More precisely, we consider an octahedron, with atomic fractional coordinates x between −0·25 and 0·25 (column A of Fig. 1). The atomic displacements are indicated in Table 4. We postulate a modulation of the

Table 3. *Fractional atomic coordinates of refined parameters*

Values indicated in Å are for strong amplitudes. Displacement factors (Å²) of the basic structure and a so-called 'average' structure (refined with main reflections) are also given.

		Basic structure	U_0	Re(U_1)	−Im(U_1)
Cd	x	0·00	0·00	0·00	0·0047 (0)
	y	0·00	0·00	0·00	0·00
	z	0·00	0·00	0·00	−0·0063 (0)
					−0·155 (1) Å
Basic		U_{11} = 0·0076 (3)	U_{22} = 0·0181 (5)	U_{33} = 0·0223 (2)	U_{13} = −0·0009 (0)
'Average'		U_{11} = 0·0084 (5)	U_{22} = 0·0195 (6)	U_{33} = 0·0336 (6)	U_{13} = −0·0040 (6)
Cl_e	x	0·25	0·00	0·00	0·0014 (1)
	y	0·25	0·00	0·00	0·0031 (2)
	z	−0·0129	0·0003 (0)	0·0081 (1)	0·00
				0·203 (3) Å	
Basic		U_{11} = 0·0152 (12)	U_{22} = 0·0244 (14)	U_{33} = 0·0350 (12)	U_{12} = 0·0076 (4)
'Average'		U_{11} = 0·0163 (13)	U_{22} = 0·0267 (15)	U_{33} = 0·0505 (20)	U_{12} = 0·0080 (11)
Cl_a	x	0·0546	−0·0007 (2)	0·00	0·0005 (2)
	y	0·00	0·00	−0·0298 (4)	0·00
				−0·219 (4) Å	
	z	0·0996	0·0006 (0)	0·00	−0·0059 (0)
					−0·148 (3) Å
Basic		U_{11} = 0·167 (11)	U_{22} = 0·0439 (17)	U_{33} = 0·0254 (17)	U_{13} = 0·0009 (1)
'Average'		U_{11} = 0·0163 (13)	U_{22} = 0·0772 (25)	U_{33} = 0·0305 (17)	U_{13} = 0·0011 (11)
N	x	0·4733	−0·0006 (11)	0·00	0·0062 (9)
	y	0·00	0·00	−0·0210 (12)	0·00
				−0·155 (9) Å	
	z	0·0855	−0·0001 (3)	0·00	−0·0019 (2)
Basic		U_{11} = 0·0216 (53)	U_{22} = 0·0524 (60)	U_{33} = 0·0191 (41)	U_{13} = −0·0057 (38)
'Average'		U_{11} = 0·0135 (46)	U_{22} = 0·0715 (73)	U_{33} = 0·0252 (53)	U_{13} = −0·0007 (40)
C(1)	x	0·5701	−0·0012 (16)	0·00	0·0113 (14)
					0·086 (11) Å
	y	0·00	0·00	−0·0027 (24)	0·00
	z	0·13893	−0·0008 (6)	0·00	−0·0028 (4)
					−0·070 (10) Å
Basic		U_{11} = 0·0338 (76)	U_{22} = 0·1344 (203)	U_{33} = 0·0259 (80)	U_{13} = −0·0058 (56)
'Average'		U_{11} = 0·0299 (64)	U_{22} = 0·1478 (173)	U_{33} = 0·0348 (85)	U_{13} = −0·0060 (60)
C(2)	x	0·4973	0·0094 (14)	0·00	−0·0369 (28)
					−0·279 (21) Å
	y	0·00	0·00	−0·0314 (42)	0·00
				−0·231 (31) Å	
	z	0·1829	−0·0019 (6)	0·00	−0·0009 (4)
Basic		U_{11} = 0·0446 (64)	U_{22} = 0·2911 (321)	U_{33} = 0·0234 (64)	U_{13} = −0·0019 (31)
'Average'		U_{11} = 0·0815 (114)	U_{22} = 0·3418 (349)	U_{33} = 0·0203 (79)	U_{13} = −0·0051 (102)
C(3)	x	0·6096	0·0010 (14)	0·00	−0·0304 (20)
					−0·230 (15) Å
	y	0·00	0·00	−0·0046 (18)	0·00
	z	0·2318	−0·0006 (5)	0·00	−0·0016 (4)
Basic		U_{11} = 0·0484 (53)	U_{22} = 0·0867 (123)	U_{33} = 0·0286 (66)	U_{13} = −0·0106 (48)
'Average'		U_{11} = 0·0809 (104)	U_{22} = 0·0933 (127)	U_{33} = 0·0294 (80)	U_{13} = −0·0178 (74)

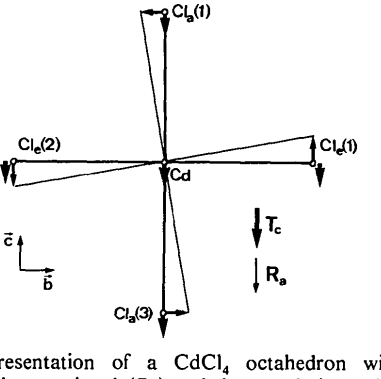

Fig. 5. Representation of a $CdCl_4$ octahedron with arrows indicating the rotational (R_a) and the translational (T_c) components of the modulation.

Table 4. *Main amplitudes of modulation of the octahedron shown in Fig. 7 as derived from Table 3*

Cd	$u_z \approx -0.16 \sin(2\pi\alpha)$
$Cl_a(1)$	$u_z \approx -0.15 \sin(2\pi\alpha)$
	$u_y \approx -0.22 \cos(2\pi\alpha)$
$Cl_a(3)$	$u_z \approx -0.15 \sin(2\pi\alpha)$
	$u_y \approx 0.22 \cos(2\pi\alpha)$
$Cl_e(1)$	$u_z \approx 0.20 \cos(2\pi\alpha + 0.21\pi)$
$Cl_e(2)$	$u_z \approx -0.20 \cos(2\pi\alpha - 0.21\pi)$

$\alpha = x_4^{Cd} = 0, \beta, 2\beta, \ldots$ for an octahedron in the A column.

Table 5. *Interatomic distances* (Å) *in the modulated phase*

	Min.	Max.		Min.	Max.
Cd–$Cl_e(1)$	2.65	2.68	N(1)–$Cl_a(1)$	3.17	3.24
Cd–$Cl_e(2)$	2.61	2.72	N(1)–$Cl_a(2)$	3.41	3.99
Cd–$Cl_a(1)$	2.54	2.55	N(1)–C(1)	1.45	1.46
$Cl_a(1)$–$Cl_e(1)$	3.50	3.88	C(1)–C(2)	1.10	1.51
			C(2)–C(3)	1.52	1.57

rotation of the octahedra around the a axis with an amplitude of approximately 5° expressed by:

$$R_a(\bar{x}_4^{Cd}) = -A_1 \cos(2\pi\bar{x}_4^{Cd}).$$

The value of A_1 corresponds to the modulation of the Cl_a atoms along the **b** direction with an amplitude of 0·22 Å.

A modulated shift of the whole octahedron having an amplitude A_2 has the form:

$$T_c(\bar{x}_4^{Cd}) = -A_2 \sin(2\pi\bar{x}_4^{Cd}).$$

The amplitude of the shift corresponds to the modulation of the Cd and Cl_a atoms along **c**. It has a value of approximately 0·15 Å (see Table 3).

If we develop the expression for the modulation at Cl_e (Table 4), we obtain:

$$\begin{aligned} Cl_e(1): \quad u_z &\approx [0.2 \text{ Å } \cos(0.21\pi)] \cos(\alpha) \\ &\quad - [0.2 \text{ Å } \sin(0.21\pi)] \sin(\alpha) \\ &\approx 0.17 \text{ Å } \cos(\alpha) - 0.13 \text{ Å } \sin(\alpha) \\ Cl_e(2): \quad u_z &\approx -0.17 \text{ Å } \cos(\alpha) - 0.13 \text{ Å } \sin(\alpha) \end{aligned}$$

where $\alpha = 2\pi\bar{x}_4^{Cd}$.

The values of 0·17 and 0·13 Å are slightly too small; however, some small amplitudes along **a** and **b** have been neglected and a simplified model of rigid octahedra has been postulated. This last hypothesis is confirmed by the interatomic distances in Table 5. The Cd–Cl bonds are nearly invariant and Cl–Cl distances do not change significantly.

If we suppose a modulation of the $Cl_e(1)$ atom having the form:

$$u_z \approx A_1 \cos(\alpha) - A_2 \sin(\alpha)$$

the values of A_1 and A_2 are related, more precisely:

$$A_2/A_1 = \tan[(\beta/2)\pi]$$

where $\beta = 0.418$ (5).

An interesting feature of this model is to exhibit the components C_1 and C_2 introduced in a two-component model of an incommensurate structure (McConnell & Heine, 1984) and expressed in the form:

$$\begin{aligned} \text{(INC structure)} = &\text{ (average structure)} \\ &+ \text{ (first component } C_1) \times \cos(2\pi\mathbf{q}.\bar{\mathbf{x}}) \\ &+ \text{ (second component } C_2) \\ &\times \sin(2\pi\mathbf{q}.\bar{\mathbf{x}}). \end{aligned}$$

C_1 corresponds to octahedra rotated by an angle of 5° (the rotational component of the modulation) and C_2 describes planes shifted by approximately 0·15 Å (the translational component of the modulation). We can easily deduce the symmetry of C_1 and C_2 by considering the elements of the superspace group leaving invariant hyperplanes defined by $\tau = 0$ and $\tau = \pi/2$ respectively (Simmons & Heine, 1987). In our case:

$$\{m_z | \tfrac{1}{2},0,\tfrac{1}{2},0\}, \{\bar{2}_z | \tfrac{1}{2},0,\tfrac{1}{2},0\}, \{E | 0,\tfrac{1}{2},\tfrac{1}{2},0\}$$

leave the hyperplane $\tau = 0$ invariant and generate $A11a$, the space group of the structure defined as (average + C_1).

$$\{m_z | \tfrac{1}{2},0,\tfrac{1}{2},0\}, \{\bar{m}_y | 0,\tfrac{1}{2},\tfrac{1}{2},\tfrac{1}{2}\}, \{E | 0,\tfrac{1}{2},\tfrac{1}{2},0\}$$

leave the hyperplane $\tau = \pi/2$ invariant and generate $A2_1ma$, the space group of the structure defined as (average + C_2).

If we consider the atoms located in column B, the symmetry element, $\{m_z | \frac{1}{2},0,\frac{1}{2},0\}$, implies a phase shift of the modulation of π. The rotation and the translation of octahedra in column B are expressed as:

$$\begin{aligned} R_a(\bar{x}_4^{Cd}) &= A_1 \cos(2\pi\bar{x}_4^{Cd}) \\ T_c(\bar{x}_4^{Cd}) &= A_2 \sin(2\pi\bar{x}_4^{Cd}). \end{aligned}$$

In other words, the displacements of connected $CdCl_6$ octahedra are opposite in phase.

5.2. *Disorder of the n-propylammonium chains*

The movement of the N–C(1)–C(2)–C(3) chain is characterized by the absence of modulation along **c**. The packing of the methyl end of the chain between two successive layers is stable: the position of C(3) does not change in the transition to the OLT phase. At the other end of the chain, the N atom shows a modulation along **b** of the same amplitude as the Cl_a atom connected to the hydrogen bond found at high temperature. This amplitude reveals a tendency to create a second stable hydrogen bond with another Cl_a atom by decreasing their interatomic distance (see Table 5). We note that if the N(1)–$Cl_a(2)$ distance is minimal, the N(2)–$Cl_a(1)$ distance is also near its minimum; this does not correspond to the hydrogen-bonding scheme observed at low temperature.

Table 5 shows that the C(2)–C(3) and N–C(1) distances are nearly invariant and chemically signifi-

cant. This is not the case for the C(2)—C(1) bond. Attempts to constrain this distance gave unsatisfactory e.s.d.'s and R values that were too high. Even at low temperature, the C(2) atom shows large disorder.

The amplitudes of N and C(2) along **b** can be considered as contributing to the C_1 component. The amplitudes of C(2) and C(3) along **a** contribute to the C_2 component.

5.3. *Basic and average structures*

The amplitudes of modulation are quite large, so it is possible to show the structural differences between the basic (or fundamental) structure and the structure derived from main reflections. For a second-order phase transition, the *basic structure* is usually defined by atoms located at the same positions $\bar{x}^\mu$ as those in the high-temperature phase. The displacement tensor is determined in a refinement procedure with main and satellite reflections. Thus, the contribution of the modulation wave to the structure factor of the main reflections is taken into account.

The *average structure* is strictly defined as the average over the internal coordinate x_4. The atoms are located at $\bar{x}^\mu + u_0^\mu$. In structural investigations we usually identify the average structure as the one determined by the refinement based on main reflections only. It is a good approximation for the atomic positions. In $(C_3H_7NH_3)_2CdCl_4$, the positions based on the refinement of the main reflections correspond (within error) to the average structure. The refined displacement parameters have, however, no physical reality, except to give some indication of the direction of the strong amplitudes of modulation [see Perez-Mato, Madariaga, Zuñiga & Garcia Arribas (1987) for further details].

Fig. 6 shows 50% thermal ellipsoids of heavy atoms corresponding to these structures. The differences between ORT structure and the 'average structure' reveal the additional disorder appearing with the modulated phase.

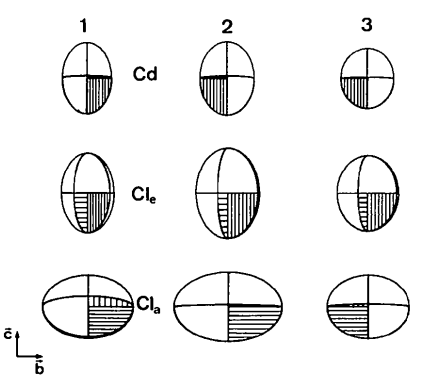

Fig. 6. Projection of Cd and Cl atoms along **a** for the ORT structure (column 1), the structure refined with main reflections (column 2) and the basic structure (column 3). Atoms are represented with 50% displacement ellipsoids.

5.4. *Lock-in transition*

At 150·0 (2) K, the satellites have maximum intensity. Lowering the temperature by ~0·5 K causes their sudden disappearance and reflections of the type $k + l = 2n + 1$ appear. This first-order phase transition can be interpreted as a lock-in transition if we admit a shift of **q** from 0·42 to **1b***. The transition from *Abma* to *Pbca* corresponds to a doubling of the primitive cell. Fig. 4 shows the differences between the diffraction patterns of the INC and OLT structures. The extinction law (0,0,l for $l = 2n$) appearing for *Pbca* is compatible with addition of structure factors of 0,0,l,m and 0,0,l,$-m$ reflections having the same magnitude but a phase difference of π. In the OLT structure, we can observe a rotation of the octahedra of approximately 10° corresponding to a possible locking of the rotational part of the modulation. The strong variation of the lattice parameter c could be connected to the translational part C_2 (see Fig. 7). As a result of

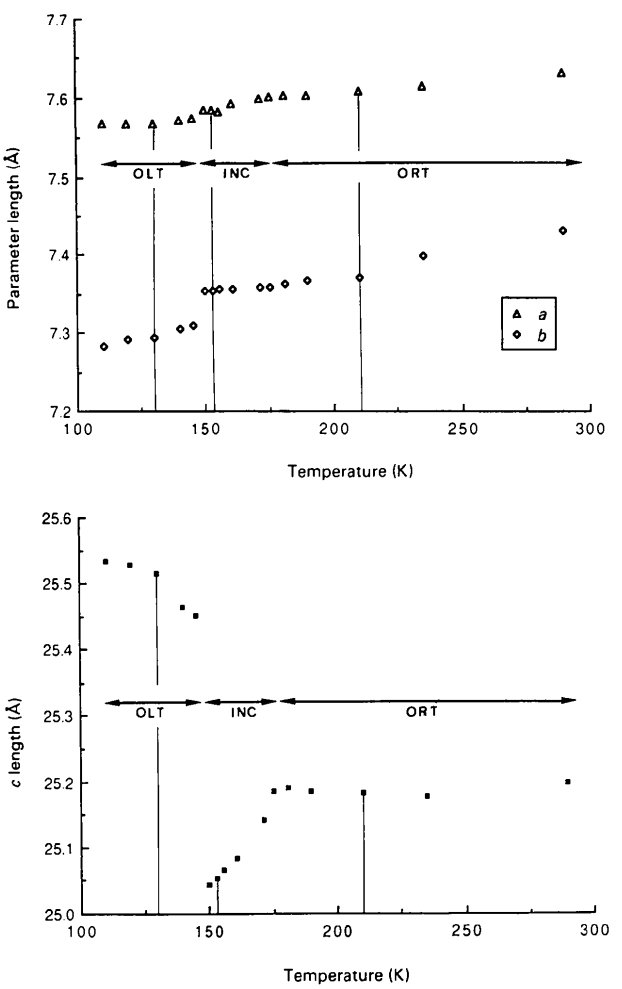

Fig. 7. Temperature variation of cell parameters a, b, c. Data collection temperatures are indicated by vertical solid lines. Magnitudes of e.s.d.'s are smaller than the printed data.

symmetry breaking, the alkylammonium chain has lost its reflection symmetry perpendicular to **b**. The chains lie mainly on the plane perpendicular to the layers of octahedra and containing the N–H···Cl_e bond.

If we consider the superspace group of the INC phase, $P^{Abma}_{s\bar{1}a}(0,\beta,0)$, with β equal to 1 ($\mathbf{q}=\mathbf{b}^*$), *Pbca* leaves invariant the structure corresponding to an internal coordinate x_4 equal to zero.

5.5 *Comparison with the* Mn *compound*

Isostructural $(C_3H_7NH_3)_2MnCl_4$ has been extensively studied by various authors. X-ray and neutron investigations (Brunskill & Depmeier, 1982; Depmeier & Mason, 1982, 1983) revealed the presence of the so-called ε phase which has strong analogies with the INC phase of $(C_3H_7NH_3)_2CdCl_4$. This phase has the same superspace group $P^{Abma}_{s\bar{1}1}(0,\beta,0)$, with $\beta=\frac{1}{3}+\delta$.

The variation of δ with temperature has been measured by neutron diffraction (Depmeier & Mason, 1983). The δ phase appearing at higher temperature also has the symmetry *Abma*. At the lock-in transition, however, the vector **q** flips to the value $\frac{1}{3}(\mathbf{b}^*-\mathbf{c}^*)$ in a monoclinic structure with space group $P2_1/b11$. Differences between $(C_3H_7NH_3)_2CdCl_4$ and $(C_3H_7NH_3)_2MnCl_4$ appear in the lock-in phase and in the temperature dependence of cell parameters. The two compounds have a lock-in transition with an abrupt variation of **q**. Some theoretical investigations using Landau theory were proposed to explain the unexpected characteristics of the incommensurate–commensurate phase transition in the Mn compound (Muralt, 1984). We expect that similar observations in $(C_3H_7NH_3)_2CdCl_4$ will confirm this theory.

No transitions corresponding to the high-temperature phases of $(C_3H_7NH_3)_2MnCl_4$ have been observed. High-temperature DSC measurements did not reveal any transitions corresponding to $\alpha\rightarrow\beta$, $\beta\rightarrow\gamma$ and $\gamma\rightarrow\delta$ of the Mn compound.

6. Conclusions

The investigation of the modulated structure of $(C_3H_7NH_3)_2CdCl_4$ has revealed some unexpected results in comparison with the usual properties of incommensurate phases:

(*a*) **q** does not vary with temperature. The value of 0·418 (5) for β remains constant within errors in a temperature range of more than 20°.

(*b*) Measurements were performed at a temperature near the lock-in transition and the harmonic approximation gives a good agreement with observations.

(*c*) A large gap between the values of β in the modulated phase and the lock-in OLT phase is observed.

The last two points indicate, perhaps, that a model based on a soliton regime near a lock-in transition would not be suitable for this compound. The ordering of hydrogen bonds is related to a rotational disorder of the $CdCl_4$ planes. Their translational disorder is related to the chain packing. The variation of the lattice constant *c* (corresponding to the interplanar distance) with temperature and its abrupt increase at the lock-in transition is another expression of this translational disorder.

Investigations of $(C_4H_9NH_3)_2CdCl_4$ to determine whether the number of C atoms is a necessary condition for the appearance of a modulated phase are in progress.

The authors wish to thank Dr A. Yamamoto for his active help and his suggestions during the refinement procedure. The help of Dr K. Schenk and Professor D. Schwarzenbach for critically reading the paper is also acknowledged.

References

AREND, H., HOFMAN, R. & WALDNER, F. (1974). *Solid State Commun.* **13**, 1629–1632.

AXE, J. D. (1980). *Phys. Rev. B*, **21**, 4181–4190.

BLINC, R., BURGAR, M., LOZAR, B., SELIGER, J., SLAK, J., RUTAR, V., AREND, H. & KIND, R. (1977). *J. Chem. Phys.* **66**, 278–287.

BRUNSKILL, I. H. & DEPMEIER, W. (1982). *Acta Cryst.* A**38**, 132–137.

CHAPUIS, G. (1978). *Acta Cryst.* B**34**, 1506–1512.

CROMER, D. T. & LIBERMAN, D. (1970). *J. Chem. Phys.* **53**, 1891–1898.

CROMER, D. T. & MANN, J. B. (1968). *Acta Cryst.* A**24**, 321–324.

DEPMEIER, W. & MASON, S. A. (1982). *Solid State Commun.* **44**, 719–722.

DEPMEIER, W. & MASON, S. A. (1983). *Solid State Commun.* **46**, 409–412.

HEINE, V. & SIMMONS, E. H. (1987). *Acta Cryst.* A**43**, 289–294.

MCCONNELL, J. D. C. & HEINE, V. (1984). *Acta Cryst.* A**40**, 473–482.

MOKHLISSE, R., COUZI, M., CHANH, N. B., HAGET, Y., HAUW, C. & MERESSE, A. (1985). *J. Phys. Chem. Solids*, **46**, 187–195.

MURALT, P. M. (1984). Thesis, ETH Zürich, Switzerland.

OVERHAUSER, A. W. (1971). *Phys. Rev. B*, **3**, 3173–3182.

PACIOREK, W. A. & KUCHARCZYK, D. (1985). *Acta Cryst.* A**41**, 462–466.

PEREZ-MATO, J. M., MADARIAGA, G., ZUÑIGA, F. J. & GARCIA ARRIBAS, A. (1987). *Acta Cryst.* A**43**, 216–226.

SIMMONS, E. H. & HEINE, V. (1987). *Acta Cryst.* A**43**, 626–635.

STEWART, J. M., KRUGER, G. J., AMMON, H. L., DICKINSON, C. W. & HALL, S. R. (1972). The *XRAY*72 system – version of June 1972. Tech. Rep. TR-192. Computer Science Center, Univ. of Maryland, College Park, Maryland, USA.

WHITE, M. A., GRANVILLE, N. W., DAVIES, N. J. & STAVELEY, L. A. K. (1981). *J. Phys. Chem. Solids*, **42**, 953–965.

WOLFF, P. M. DE, JANSSEN, T. & JANNER, A. (1981). *Acta Cryst.* A**37**, 625–636.

YAMAMOTO, A. (1982). *Acta Cryst.* A**38**, 87–92.

YAMAMOTO, A. (1987). Private communication.

YAMAMOTO, A., NAKAZAWA, H., KITAMURA, M. & MORIMOTO, N. (1984). *Acta Cryst.* B**40**, 228–237.